Histologic and Dynamic Changes Induced by Chronic Metabolic Acidosis in the Rat Growth Plate

EDUARDO CARBAJO,* JOSÉ MANUEL LÓPEZ,† FERNANDO SANTOS,‡ FLOR ANGEL ORDÓÑEZ,‡ PILAR NIÑO,* and JULIÁN RODRÍGUEZ‡

*Departments of *Anatomy, †Cell Biology, and ‡Pediatrics, IUOPA, School of Medicine, Hospital Central de Asturias, University of Oviedo, Oviedo, Asturias, Spain.*

Abstract. To understand better the pathophysiology of growth impairment in persistent metabolic acidosis, the morphology and dynamics of the growth plate were studied in young rats grouped as follows: rats that were made acidotic by oral administration of ammonium chloride for 14 d (AC), nonacidotic rats that were fed *ad libitum* (control [C]), and nonacidotic rats that were pair-fed with the AC group (PF). AC rats became markedly acidotic and growth retarded. The volume of newly formed bone per day (mean ± SEM) was significantly lowered ($P < 0.05$) in AC rats (AC, 3.4 ± 0.4; C, 8.4 ± 0.6; PF, 6.4 ± 0.5 mm^3/d). Growth plate height was lower in AC rats (303.8 ± 12.7 μm) than in either C (478.0 ± 16.0 μm) or PF rats (439.0 ± 21.4 μm). The processes of chondrocyte proliferation (assessed by bromodeoxyuridine labeling) and maturation (assessed by stereologic estimators of size and shape of chondrocytes and the volume of matrix per cell) were not impaired by acidosis. By contrast, the dynamics of hypertrophic chondrocytes were altered significantly: both cell turnover per column per day (AC, 4.4 ± 0.4; C, 8.0 ± 0.8; PF, 6.2 ± 0.6) and linear velocity of advance of chondrocytes (AC, 5.7 ± 0.5; C, 11.2 ± 0.9; PF, 9.4 ± 0.8 μm/h) were lowered significantly. The study presented here shows the inhibitory effect of metabolic acidosis on cartilage cell progression and endochondral bone formation. Finally, the data show that metabolic acidosis caused a marked shortening of the growth plate because chondrocyte turnover was affected to a greater extent than bone tissue formation.

Chronic metabolic acidosis is a common manifestation of renal disease, such as renal failure and renal tubular acidosis. Sustained metabolic acidosis stunts growth (1–3), but the pathogenesis of this growth retardation is not understood fully. Reduced food intake, increased protein catabolism, acidotic state itself, and growth hormone/insulin-like growth factor-1 dysfunction have been implicated as pathogenic factors (4–8).

The modifications induced by chronic renal failure and malnutrition on the growth plate of long bones (9–11), the effector organs of longitudinal growth (12,13), have been studied recently. It is of note that despite that metabolic acidosis frequently is associated with these disorders, no data are available on the modifications induced by chronic metabolic acidosis on the structure and dynamics of the growth plate.

Longitudinal bone growth is a complex phenomenon that results from progressive replacement of growth plate cartilage by osseous tissue at the metaphysis. Proliferation and hypertrophy of chondrocytes and matrix synthesis are the main events that sustain growth at the epiphysial plate (13,14). Therefore, a detailed study of the morphology and dynamics of the growth plate in the presence of persistent metabolic acidosis will add to our understanding of the pathophysiology of growth impairment in this disorder. Accordingly, we used stereologic and cytodynamic techniques to analyze the characteristics and activity of chondrocytes in the growth plate of young rats with growth retardation secondary to metabolic acidosis.

Materials and Methods

Animals and Experimental Protocol

Female Sprague Dawley rats (65 ± 5 g of body wt and 25 ± 3 d of age) were obtained from the breeding area of the animal facility building of the University of Oviedo. Rats were housed in individual cages in a light- and temperature-controlled environment (12 h light-dark cycle; 22 ± 1°C) and received standard 23.9% protein rat chow (AO3, Panlab SL, Barcelona, Spain) and tap water. After 3 d of adaptation to the experimental area, the rats were classified into three groups of five rats each (day 0 of the protocol): acidotic rats (AC), rats that were pair-fed with AC (PF), and control rats that were fed *ad libitum* (C). Acidosis was induced by daily administration of ammonium chloride (NH_4Cl) as drinking solution at progressively increased concentrations of 1.8% (days 0 to 5), 2.0% (days 6 to 10), and 2.2% (days 11 to 14).

Rats' weight as well as chow and water consumption were measured daily with an electronic balance Ohaus GT 2001 (Ohaus Scale Corp., Florham Park, NJ). Nose to tip tail length was measured under anesthesia on days 0 and 14. Food efficiency was calculated as grams of weight gained per gram of food consumed. On day 14, rats were killed by exsanguination under anesthesia with methoxyflurane. All rats received intraperitoneal injections of calcein (Sigma, St. Louis, MO; 15 mg/kg body wt) and 5-bromo-2'-deoxyuridine (BrdU; Sigma; 100 mg/kg body wt) 4 d and 1 h before being killed, respectively.

Received May 22, 2000. Accepted November 21, 2000.
Correspondence to Dr. Eduardo Carbajo, Anatomía, Facultad de Medicina, C/Julián Clavería s/n, 33006 Oviedo, Asturias, Spain. Phone: 34-98-510-3585; Fax: 34-98-510-3585; E-mail: ecp3@correo.uniovi.es
1046-6673/1206-1228
Journal of the American Society of Nephrology

Blood acid-base equilibrium was determined with a Ciba-Corning 855 gas analyzer (Ciba-Corning Diagnostics Corp., Medfield, MA).

Tissue Collection and Processing

Tibiae were isolated immediately after death. Soft tissues were removed, and tibia lengths and frontal and sagittal diameters at the level of the upper growth plates were measured with the use of a sliding mechanical caliper (accuracy, 0.01 mm). Frontal and sagittal diameters were used for estimation of the growth plate area perpendicular to the long axis, horizontal projection area, according to the ellipse formula (15). Blocks from proximal tibial growth plates were chosen by a systematic random-sampling process reported previously (10). Two blocks were used for measurement of the rate of longitudinal bone growth, two blocks were used for histomorphometric analysis, and one block was used for immunocytochemical identification of proliferating chondrocytes.

The tissue processing procedure has been described (10). Briefly, tissue blocks for determination of longitudinal bone growth rate were fixed in 40% ethanol, dehydrated in ethanol, and embedded in Durkupan-ACM (Sigma). Tissue blocks for histomorphometry were transferred immediately to 2% glutaraldehyde solution containing 0.7% ruthenium hexamine trichloride (Strem Chemicals, Newburyport, MA) for 3 h, transferred to 1% osmium tetroxide and 0.7% ruthenium hexamine trichloride for 2 h, dehydrated in ascending concentrations of acetone, and embedded in Durkupan-ACM. Tissue blocks for immunocytochemical identification of proliferating chondrocytes were fixed in a mixture of 0.5% glutaraldehyde and 4% paraformaldehyde, dehydrated in ascending concentrations of acetone, and embedded in Durkupan-ACM.

Embedded tissues were cut on a Reicher Ultracut E ultramicrotome (Leica Microsistemas S.A., Barcelona, Spain) parallel to the tibial vertical axis, with the section angle oriented randomly relative to the horizontal plane for each block. The mean thickness of the sections, analyzed under a JEOL JEM-2000 EX II electron microscope (Izasa-Rego, Barcelona, Spain), was 1.08 ± 0.04 (SD) μm.

Determination of Longitudinal Bone Growth Rate

Sections were examined under a Leitz incident light fluorescence microscope (Leica Microsistemas S.A.), and the distance between the zone of vascular invasion and the proximal part of the calcein label was measured with an eyepiece micrometer (16). Measurements were obtained at three locations, determined in an unbiased manner, on each of the four sections per rat, and the mean of these measurements divided by 4 (d) was considered as the longitudinal bone growth per day in each rat. The volume of newly formed bone per day also was calculated by multiplying the longitudinal bone growth per day by the growth plate area perpendicular to the long axis of the tibia (17).

Immunocytochemical Identification of Proliferating Chondrocytes

As described elsewhere (10), semithin sections were etched in 50% sodium ethoxide and incubated overnight with an anti-BrdU monoclonal antibody (1:20; Dakopatts, Glostrup, Denmark). This was followed by incubation with biotinylated anti-mouse IgG for 60 min (Biomeda Corp., Foster City, CA) and streptavidin-peroxidase complex (45 min at room temperature). The final reaction product was developed by incubation with 3,3'-diaminobenzidine. Proliferative activity was quantified by the estimation of the labeling index, which was defined as the percentage of BrdU-labeled cells within the proliferative stratum.

Histomorphometry

Sections were stained with toluidine blue and photographed under the light microscope first at low magnification (×230). On these low-magnification prints, growth plates were divided into stem cell, proliferating, and hypertrophic zones defined according to morphologic criteria (15). The height of the proliferative zone was calculated as the mean of three different measurements performed at three locations chosen randomly on each section. The heights of the growth plate and its different zones were estimated by point counting from the height of the proliferative zone. The volume of the growth plate and the volume of the different zones were estimated by multiplying the horizontal projection area by the mean growth plate height and the mean height of the different zones, respectively.

From each section, two quadrants from the proliferating zone and one from the hypertrophic zone were sampled, photographed, and printed on paper with a final magnification factor of ×700. The following stereologic estimators were determined within each zone: volume fraction of chondrocytes, numeric density of chondrocytes, total number of chondrocytes, mean chondrocyte volume, mean matrix volume per chondrocyte, mean projected horizontal diameter, mean chondrocyte height, number of chondrocytes in a vertical cell column, and growth fraction. Estimation of these parameters was performed as described in detail elsewhere (10). Examination of the sections and photographs always was performed by the same investigator in a blinded manner (unaware of to which group the material under study belonged). All measurements were done three times, and means and SD were calculated. SD always was less than 10%. The mean values so obtained were used to calculate the final estimates.

Table 1. Body and bone growth data (± SEM) in acidotic and nonacidotic rats, either fed *ad libitum* or pair fed with the acidotic group[a]

Parameter	C	PF	AC
Weight gain (g)	91.6 ± 4.6	40.4 ± 5.8[b]	14.7 ± 4.9[b,c]
Length gain (cm)	9.1 ± 0.1	6.0 ± 0.2[b]	3.9 ± 0.4[b,c]
Tibial length (mm)	32.4 ± 0.2	31.6 ± 0.2[b]	29.6 ± 0.2[b,c]
Horizontal projection area of growth plate (mm^2)	31.4 ± 0.7	31.2 ± 1.7	24.6 ± 0.8[b,c]
Longitudinal growth rate (μm/d)	269 ± 9	204 ± 5[b]	138 ± 13[b,c]
Volume of newly formed bone (mm^3/d)	8.4 ± 0.6	6.4 ± 0.5[b]	3.4 ± 0.4[b,c]

[a] AC, acidotic rats; C, nonacidotic control rats fed *ad libitum*; PF, nonacidotic rats pair-fed with AC group.
[b] $P < 0.05$ compared with C.
[c] $P < 0.05$ compared with PF.

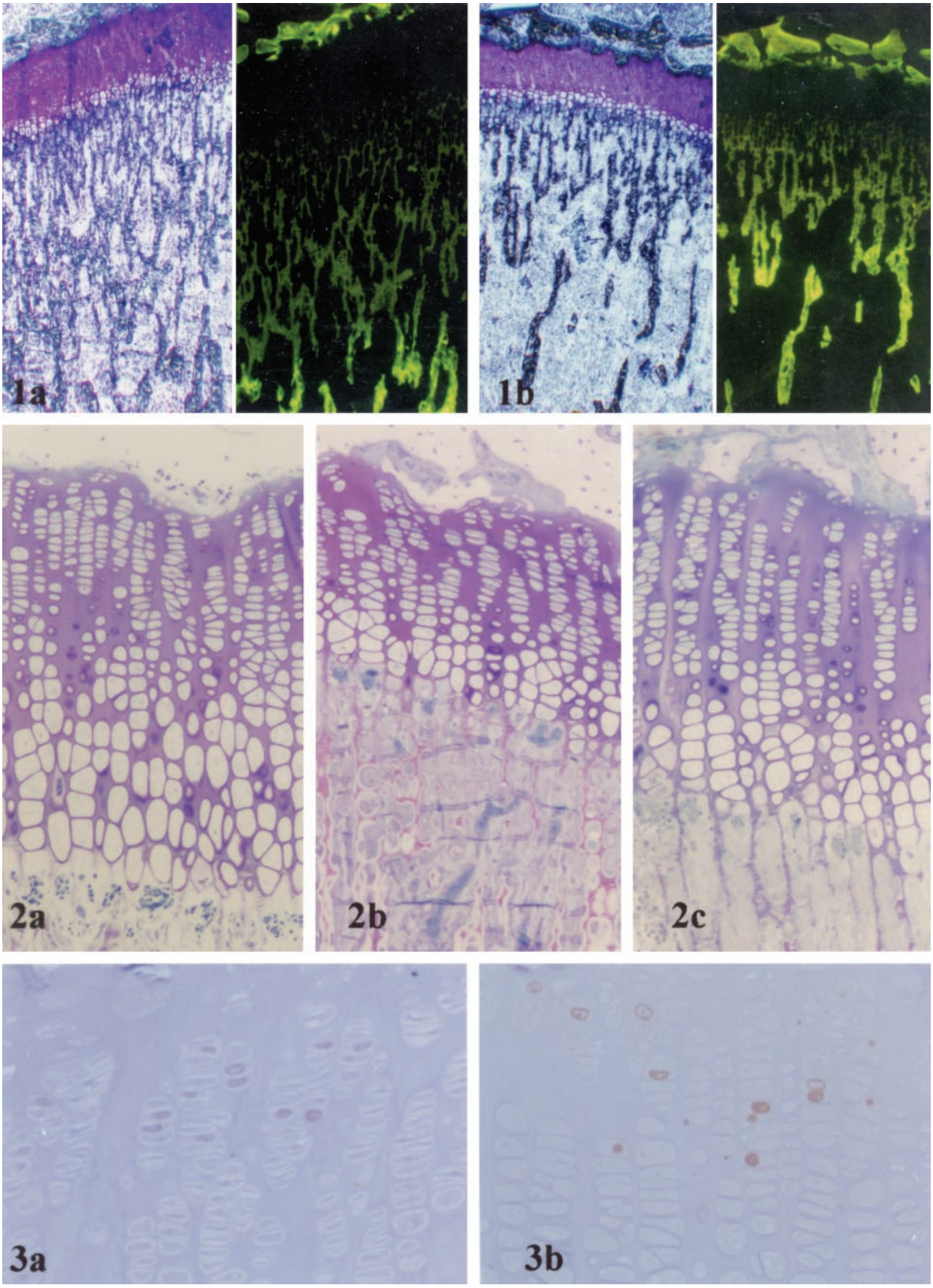

Figure 1. Parallel sections of the proximal tibial growth plates of control (C) rats (a) and acidotic (AC) rats (b) examined by bright field microscopy after toluidine blue staining (*left*) and by incident-light fluorescence microscopy (*right*). The distance between the lower border of the growth plate and the fluorochrome-labeled front clearly is longer in C than in AC rats. Magnification, ×50.

The minimum number of points to be analyzed was determined according to Cruz-Orive and Hunziker (15).

Cell Kinetics

Growth plate over a short time period (such as 4 d, the time interval established here to calculate longitudinal growth) can be considered a steady state system in which cell production and elimination rates as well as growth plate height are constant (18). On this basis, the mean cell turnover per column per day, the turnover time, and the linear velocity of advance of chondrocytes in the columns were estimated as described previously (10).

Statistical Analyses

Values of each group are given as mean ± SEM. For the growth plate data, a mean value for each of the tested parameters was calculated on a per-rat basis in the group. Then, each rat was considered a sample for statistical purposes. The data obtained were shown to follow a normal distribution with homogeneity of variances and independence. Comparison among the three groups was performed by ANOVA, with the use of a significance level of 95%, followed by the Newman-Keuls multiple range test.

Results

The administration of NH_4Cl induced a severe metabolic acidosis as documented by the significant ($P < 0.05$) reduction in the serum total CO_2 of AC rats (13.4 ± 0.7 mM/L), compared with C rats (24.4 ± 0.9 mM/L) and PF rats (25.2 ± 1.1 mM/L). Mean daily food intake of AC rats (9.2. ± 0.3 g) and, therefore, of PF rats was approximately 60% of that of C rats (16.2 ± 0.2 g). The metabolic acidosis was associated with growth retardation as demonstrated by weight and length gains, tibial length, rate of longitudinal growth, and volume of newly formed bone per day (Table 1). All of these parameters were was significantly lower in AC rats than in any of the groups of nonacidotic rats (C, PF). In turn, PF rats grew less than C rats.

Under the light microscope, the growth plate of AC rats was shorter in height than that of either PF or C rats (Figures 1 and 2). The columnar organization of the growth plate was well preserved in the three groups of rats, the interface between the growth plate cartilage and the metaphysial bone was well defined, and a common pattern of invading capillary vessels was clearly identifiable.

Stereologic parameters describing the features of the growth plate cartilage and chondrocytes are given in Tables 2 and 3, respectively. The height of the entire growth plate was significantly lower in AC rats than in either of the nonacidotic groups of rats. The shortening of the growth plate in AC rats was due mainly to a decreased height of the hypertrophic zone (approximately 50% of that of C rats) and, to a lesser extent, the reduction in height of the proliferative zone (approximately 70% of that of C rats). No differences between groups were observed in the volume fraction or the numeric density of chondrocytes, but the total number of chondrocytes in the proliferative and hypertrophic zones of the AC group was lower than in either of the other two groups.

Table 2. Stereologic estimators (± SEM) of the proximal tibial growth plate in AC rats and C or PF rats

Parameter	C	PF	AC
Growth plate height (μm)			
global	478 ± 16	439 ± 21	304 ± 13[a,b]
resting zone	29 ± 1	25 ± 2	32 ± 3
proliferating zone	181 ± 7	165 ± 4	137 ± 2[a,b]
hypertrophic zone	268 ± 10	249 ± 21	135 ± 11[a,b]
Growth plate volume (mm^3)			
global	15.0 ± 0.5	13.6 ± 0.4	7.5 ± 0.4[a,b]
resting zone	0.9 ± 0.1	0.8 ± 0.1	0.8 ± 0.1
proliferating zone	5.7 ± 0.3	5.8 ± 0.3	3.4 ± 0.1[a,b]
hypertrophic zone	8.4 ± 0.3	7.1 ± 0.5	3.3 ± 0.3[a,b]
Volume fraction of chondrocytes (%)			
resting zone	20.8 ± 1.7	26.2 ± 3.2	22.7 ± 3.3
proliferating zone	36.3 ± 3.8	39.1 ± 1.1	34.0 ± 0.3
hypertrophic zone	62.1 ± 4.2	58.6 ± 4.7	56.0 ± 3.2
Numerical density of chondrocytes (no. of cells × $10^3/mm^3$ of tissue)			
resting zone	154 ± 10	153 ± 11	143 ± 10
proliferating zone	230 ± 18	212 ± 21	203 ± 17
hypertrophic zone	48 ± 5	52 ± 6	54 ± 8
Total number of chondrocytes ($\times 10^3$)			
resting zone	137 ± 8	1219	112 ± 7
proliferating zone	1307 ± 104	1226 ± 124	689 ± 59[a,b]
hypertrophic zone	406 ± 44	366 ± 45	178 ± 26[a,b]

[a] $P < 0.05$ compared with C.
[b] $P < 0.05$ compared with PF.

Structural parameters (Table 3), related either to size (mean cell volume) or shape (mean projected horizontal diameter, mean height of cell profile) of chondrocytes, did not differ among groups. No differences were found for the ratio matrix volume per chondrocyte or for the mean number of chondrocytes per column.

Proliferative activity of chondrocytes did not differ significantly among groups (Table 4). Regardless of the group, the distribution of BrdU-labeled chondrocytes was fairly heterogeneous (Figure 3), although labeled cells were confined to the proliferative zone. As for other kinetic parameters, the growth fraction showed no differences among the three groups of rats. However, the cell turnover per column per day clearly was reduced in AC rats compared with either of the nonacidotic

Figure 2. Light micrographs of vertical semithin sections of the proximal tibial growth plate of C (a), AC (b), and pair-fed (PF) rats (c). The growth plate clearly was shorter in AC rats than in any other group, mainly as a result of a relative shortening of the hypertrophic zone. Magnification, ×160 (toluidine blue staining).

Figure 3. 5-Bromo-2'-deoxyuridine–labeled cells in the proximal tibial growth plate of C (a) and AC (b) rats. Sections counterstained with hematoxylin. Magnification, ×350.

Table 3. Growth plate chondrocyte structural parameters (± SEM) in AC rats and C or PF rats

Parameter	C	PF	AC
Mean cell volume (μm^3)			
proliferating zone	1580 ± 90	1840 ± 97	1678 ± 111
hypertrophic zone	12911 ± 1112	11312 ± 1098	10448 ± 1098
Mean matrix volume per cell (μm^3)			
proliferating zone	2773 ± 250	2866 ± 266	3258 ± 203
hypertrophic zone	7879 ± 547	7992 ± 1076	8209 ± 1043
Mean projected horizontal diameter (μm)			
proliferating zone	15.7 ± 0.9	16.1 ± 1.1	16.2 ± 1.2
hypertrophic zone	26.5 ± 3.8	28.3 ± 4.1	27.9 ± 3.9[a,b]
Mean cell height (μm)			
proliferating zone	8.1 ± 1.1	8.3 ± 1.2	8.2 ± 1.0
hypertrophic zone	33.4 ± 4.5	32.8 ± 5.1	31.5 ± 5.3
Number of chondrocytes in a cell column			
global	31.3 ± 4.7	27.4 ± 6.2	21.0 ± 3.9
proliferating zone	23.3 ± 3.5	19.8 ± 4.1	16.7 ± 1.8
hypertrophic zone	8.0 ± 1.2	7.6 ± 2.1	4.3 ± 0.8

[a] $P < 0.05$ compared with C.
[b] $P < 0.05$ compared with PF.

groups. Estimation of daily rates of cellular turnover showed that cell columns eliminate approximately 8 chondrocytes per day (1 chondrocyte every 3 h) in C rats and 6.2 or 4.4 cells per day (1 chondrocyte every 3.9 or 5.5 h, respectively) in PF and AC rats. Changes in cell turnover were not accompanied by modifications in the duration of the hypertrophic activity phase, but the linear velocity of advance of chondrocytes in the vertical columns decreased significantly in AC rats when compared with either PF or C rats.

Discussion

In the study presented here, growth impairment induced by acidosis likely was the result of the combined effect of reduced food intake and the acidotic state itself because AC rats grew less than PF rats, and, in turn, this group with a normal acid-base balance gained less weight and length than C rats. As also shown in Table 1, differences in body growth paralleled those found in tibial length, longitudinal bone growth rate, and volume of recently formed bone.

More interesting, chronic metabolic acidosis caused significant alterations in the growth plate that were not present in the two groups of nonacidotic rats. As shown in Table 2, the tibial growth plate of AC rats was much smaller, as confirmed by a markedly reduced height and volume, than that of PF and C rats. Growth plates of PF and C rats had a similar size. Elongation of long bones is the result of the interplay of two coupled processes: continual and vectorial production of cartilage by the growth plate and replacement of cartilage by bone tissue at the epiphysial/metaphysial interface. A strict coordination among the processes of cartilage enlargement, cartilage resorption, and osseous tissue formation at the metaphysial end is required for normal bone growth. Thus, the association of stunted longitudinal growth and reduced growth plate height found in the AC rats indicates a disruption of this equilibrium because cartilage production and bone formation both were decreased, although at different intensity. In these rats, the production of cartilage was slowed significantly through the replacement of cartilage by bone, resulting in a shortened growth plate. Our study shows that the chondrocyte advance and its turnover (Table 4), as well as the formation of osseous

Table 4. Growth plate chondrocyte kinetic parameters (± SEM) in AC rats and C or PF rats

Parameter	C	PF	AC
BrdU[a]-labeling index (%)	17.3 ± 2.2	14.5 ± 2.1	12.8 ± 1.9
Growth fraction (%)	73.6 ± 7.4	72.3 ± 6.6	79.6 ± 8.2
Cell turnover per column per day	8.0 ± 0.8	6.2 ± 0.6	4.4 ± 0.4[b,c]
Duration hypertrophic phase (h)	24.0 ± 2.0	26.6 ± 2.3	23.5 ± 2.0
Cellular advance velocity (μm/h)	11.2 ± 0.9	9.4 ± 0.8	5.7 ± 0.5[b,c]

[a] BrdU, 5-bromo-2′-deoxyuridine.
[b] $P < 0.05$ compared with C.
[c] $P < 0.05$ compared with PF.

tissue (Table 1), were lower in the AC rats, demonstrating the inhibitory effect of metabolic acidosis on cartilage cell progression and endochondral bone formation. Thus, the decreased height of the growth plate induced by acidosis was the result of alterations at both sides of the calcification front. *In vitro* studies (19,20) showed that acidosis exerts a direct effect on bone cells, suppressing synthesis of collagen and alkaline phosphatase activity in osteoblasts and stimulating osteoclastic bone resorption. Therefore, the reduction of daily bone formation observed in our AC rats may be linked to a decreased collagen synthesis.

Our study also indicates that the processes of chondrocyte proliferation, as assessed by the BrdU labeling index, and maturation, as assessed by stereologic estimators of size and shape of chondrocytes and the volume of matrix per cell, were not impaired by acidosis (Tables 2 and 3). It has been shown that growth may be disturbed severely in the presence of normal cartilage cell proliferation at the growth plate (12,21), and, in agreement with the present results, growth plate chondrocytes of growth-retarded uremic rats have been shown to have normal proliferative activity (10). However, the preserved morphology of chondrocytes at the different stages of their progression through the growth plate was a finding essentially dissimilar to that found in other metabolic and renal disorders associated with an altered process of chondrocyte maturation, such as vitamin D–deficient rickets (22) and severe chronic renal failure (10). In rachitic rats, the hypertrophic chondrocytes become much bigger than normal, whereas the hypertrophic chondrocytes of uremic rats are abnormally small. Like the acidotic rats, knockout of the *PTHrP* gene causes very short growth plates, but in these transgenic mice, the chondrocytes do not proliferate normally and the process of chondrocyte differentiation is accelerated so that their extracellular matrix is mineralized prematurely and the cells undergo early apoptosis (23,24). Although markers of chondrocyte differentiation, *e.g.*, type X collagen synthesis, were not analyzed, the stereologic analysis performed in our study suggests that the process of chondrocyte maturation was unaltered in the AC rats. Therefore, the mechanism responsible for the slowed transit of chondrocytes along the growth plate remains to be established. Because the movement of chondrocytes is not passive but requires vectorial degradation of matrix at the metaphysial cell pole and resynthesis at the epiphysial cell pole, it is tempting to speculate that acidosis impairs this process of matrix remodeling at the hypertrophic zone of the growth plate. Evidence supporting this hypothesis clearly deserves further investigation.

In conclusion, our study characterizes, for the first time, the modifications caused by sustained metabolic acidosis in the young rat's growth plate. In addition, our findings suggest that acidosis is not the main pathogenic factor responsible for the marked impairment of chondrocyte maturation found in the growth plate of severely uremic animals (10).

Acknowledgment

This research was supported by grant PM96-0110 from the Dirección General de Investigación Científica y Técnica del Ministerio de Educación y Cultura.

References

1. Cooke RE, Boyden DG, Haller E: The relationship of acidosis and growth retardation. *J Pediatr* 57: 326–337, 1960
2. Santos F, Chan JCM: Renal tubular acidosis in children. *Am J Nephrol* 6: 289–295, 1996
3. Maniar S, Caldas A, Laouari D, Kleinkecht C: Severity of chronic metabolic acidosis and growth of rats with chronic uremia. *Miner Electrolyte Metab* 18: 241–244, 1992
4. McSherry E: Acidosis and growth in no uremic renal disease. *Kidney Int* 14: 349–354, 1978
5. McSherry E, Morris RC Jr: Attainment and maintenance of normal stature with alkali therapy in infants and children with classic renal tubular acidosis. *J Clin Invest* 61: 509–527, 1978
6. Potter DE, Greifer I: Statural growth of children with renal disease. *Kidney Int* 14: 334–339, 1978
7. Challa A, Chan W, Krieg RJ Jr, Thabet MA, Liu F, Hintz RL, Chan JCM: Effect of metabolic acidosis on the expression of insulin-like growth factor and growth hormone receptor. *Kidney Int* 44: 1224–1227, 1993
8. McSherry E: Renal tubular acidosis in childhood. *Kidney Int* 20: 799–809, 1981
9. Cobo A, Carbajo E, Santos F, García E, López JM: Morphometry of uremic rat growth plate. *Miner Electrolyte Metab* 22: 192–195, 1996
10. Cobo A, López JM, Carbajo E, Santos F, Alvarez J, Fernández M, Weruaga A: Growth plate cartilage formation and resorption are differentially depressed in growth retarded uremic rats. *J Am Soc Nephrol* 10: 971–979, 1999
11. Sanchez CP, Salusky IB, Kuizon BD, Abdella P, Juppner H, Goodman WG: Growth of long bones in renal failure: Roles of hyperparathyroidism, growth hormone and calcitriol. *Kidney Int* 54: 1879–1887, 1998
12. Breur GJ, Farnum CE, Padgett GA, Wilsman NJ: Cellular basis of decreased rate of longitudinal growth of bone in pseudoachondroplastic dogs. *J Bone Joint Surg Am* 74: 516–528, 1992
13. Hunziker EB: Mechanism of longitudinal bone growth and its regulation by growth plate chondrocytes. *Microsc Res Tech* 28: 505–519, 1994
14. Mehls O, Ritz E, Hunziker EB, Eggli P, Heinrich U, Zapf J: Improvement of growth and food utilization by human recombinant growth hormone in uremia. *Kidney Int* 33: 45–52, 1988
15. Cruz-Orive LM, Hunziker EB: Stereology for anisotropic cells: Application to growth cartilage. *J Microsc* 143: 47–80, 1986
16. Hansson LI, Menander-Sellman K, Stenstrom A, Thorngren KG: Rate of normal longitudinal bone growth in the rat. *Calcif Tissue Res* 10: 238–251, 1972
17. Breur GJ, Turgai J, Vanenkevort BA, Farnum CE, Wilsman NJ: Stereological and serial section analysis of chondrocytic enlargement in the proximal tibial growth plate of the rat. *Anat Rec* 239: 255–268, 1994
18. Hunziker EB, Schenk RK: Physiological mechanisms adopted by chondrocytes in regulating longitudinal bone growth in rats. *J Physiol* 414: 55–71, 1989
19. Krieger NS, Sessler NE, Bushinsky DA: Acidosis inhibits osteoblastic and stimulates osteoclastic activity in vitro. *Am J Physiol* 262: F442–F448, 1992

20. Bushinsky DA: Stimulated osteoclastic and suppressed osteoblastic activity in metabolic but not respiratory acidosis. *Am J Physiol* 268: C80–C88, 1995
21. Hunziker EB, Wagner J, Zapf J: Differential effects of IGF-I and hGH on the various developmental stages of growth plate chondrocytes in vitro. *J Clin Invest* 93: 1078–1086, 1994
22. Dean DD, Muñiz OE, Berman I, Pita JC, Carreño MR, Woessner JF, Howell DS: Localization of collagenase in the growth plate of rachitic rats. *J Clin Invest* 76: 716–722, 1984
23. Karaplis AC, Luz A, Glowacki J, Bronson RT, Tybulewicz VL, Kronenberg HM, Mulligan RC: Lethal skeletal dysplasia from targeted disruption of the parathyroid hormone-related peptide gene. *Genes Dev* 8: 277–289, 1994
24. Amizuka N, Henderson JE, Hoshi K, Warshawsky H, Ozawa H, Goltzman D, Karaplis AC: Programmed cell death of chondrocytes and aberrant chondrogenesis in mice homozygous for parathyroid hormone-related peptide gene deletion. *Endocrinology* 137: 5055–5067, 1996